Analysis of diffractions in dip-angle gathers for transversely isotropic media

Yogesh Arora and Ilya Tsvankin
Center for Wave Phenomena, Colorado School of Mines

Key words: Diffractions, transverse isotropy, dip-angle gathers, diffraction imaging

ABSTRACT
Diffractions can supplement reflected waves in anisotropic velocity analysis because they increase the aperture and may illuminate parts of the model that do not produce strong reflections. However, enhancement of diffractions and their separation from the more intensive reflections remains a challenging task, especially if the velocity model is not sufficiently accurate. Here, we construct dip-angle common-image gathers (CIGs) for transversely isotropic (TI) media using Kirchhoff migration. Dip-angle gathers can be conveniently used to generate diffraction-based depth images if a sufficiently accurate velocity model is available. We also analyze the moveout distortions of diffraction and reflection events in dip-angle CIGs in the presence of errors in the TI parameters. The residual moveout of diffractions computed from dip-angle gathers can be employed in migration velocity analysis (MVA) to refine the anisotropic velocity model.

1 INTRODUCTION

Diffractions can be helpful in anisotropic parameter estimation because they carry information from a wide range of propagation angles (e.g., Waheed et al., 2013a,b) and for spatial locations often not illuminated by reflections. Diffraction events produced by discontinuities (e.g., faults, fractures, and other geologic features) and strong heterogeneities have been employed to refine isotropic velocity models. For example, local slant-stacks (Harlan et al., 1984) and the minimum entropy (ME) norm (De Vries and Berkhout, 1984) were applied to focus diffractions on common-offset (poststack) sections and perform isotropic velocity analysis. Söllner et al. (2002) extend the focusing-based normal-moveout velocity analysis of diffractions to 3D common-offset sections. Fomel et al. (2007) use a velocity-continuation method for migration velocity analysis (MVA) of zero-offset diffraction time images. Techniques designed to incorporate reflections and diffractions simultaneously into isotropic velocity analysis include 2D stereotomography (Billette et al., 2003) and wave-equation MVA (Sava et al., 2005).

One of the main challenges in utilizing diffractions for velocity analysis is their separation from reflections, which usually dominate surface seismic data (e.g., Klem-Musatov et al. 1994). Existing methodologies for diffraction separation are mostly limited to isotropic media and require accurate velocity models (Khaidukov et al., 2004; Kozlov et al., 2004; Berkovitch et al., 2009; Moser and Howard, 2008; Sturzu et al., 2013). Arora and Tsvankin (2016) develop a specularity-based method for separating diffractions in anisotropic media and apply it to 2D VTI (TI with vertical symmetry axis) media. Images of diffracted energy can supplement reflection-based interpretation in applications such as fracture characterization (Al-Dajani and Fomel, 2010) and time-lapse seismic monitoring (Alonaizi et al., 2014).

Producing well-focused depth images from diffractions typically requires model updating through migration velocity analysis. Audebert et al. (2002) introduce the so called dip-angle CIGs, in which the distinct signature of diffractions can help separate them from reflections (Landa et al., 2008). Also, similar to reflections in surface-offset-based gathers, diffraction events exhibit residual moveout in dip-angle gathers when the velocity model is inaccurate. The possibility of performing diffraction-based isotropic MVA of poststack data in the dip-angle domain is explored by Reshef and Landa (2009) and Klokov and Fomel (2012).

Here, we compute dip-angle CIGs from prestack reflection data in TI media using Kirchhoff depth migration. First, we describe a methodology for constructing dip-angle CIGs and analyze the signatures of both reflections and diffractions in that domain. Then diffraction-based depth images are produced using dip-angle gathers computed for a VTI ramp model. Finally, we analyze the sensitivity of diffraction and reflection events in dip-angle CIGs to errors in the interval parameters of layered VTI media and discuss the possibility of refining the

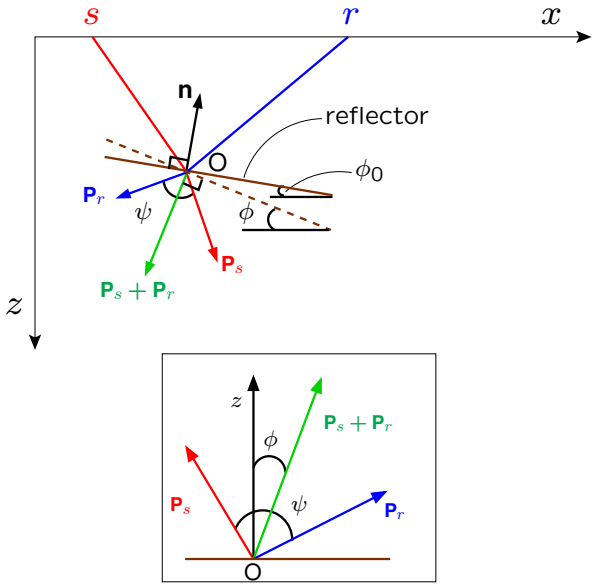

Figure 1. Image point O on a dipping reflector (dip ϕ_0) for a certain source (s) − receiver (r) pair. $\mathbf{P}_\mathrm{s}$ and $\mathbf{P}_\mathrm{r}$ denote the source- and receiver-side slowness vectors, and **n** is the reflector normal. The migrated dip ϕ corresponds to the direction (dashed line) orthogonal to the vector $\mathbf{P}_\mathrm{s} + \mathbf{P}_\mathrm{r}$. The inset shows the scattering (ψ) and migration-dip (ϕ) angles.

anisotropic velocity model by minimizing the residual moveout of diffractions.

2 CONSTRUCTION OF DIP-ANGLE CIGS AND DIFFRACTION-BASED IMAGES

In 2D Kirchhoff migration, the contributions of available seismic traces at any image point (**X**) can be described by summation over the so called migration-dip and scattering angles (Bleistein et al., 2013). The angle between the source-side slowness vector ($\mathbf{P}_\mathrm{s}$) and the receiver-side slowness vector ($\mathbf{P}_\mathrm{r}$) is called the scattering angle (ψ) (Figure 1). The sum of the slowness vectors ($\mathbf{P}_\mathrm{s} + \mathbf{P}_\mathrm{r}$) represents the migration-dip direction (Audebert et al., 2002; Brandsberg-Dahl et al., 2003), which is aligned with the interface normal for specular reflections migrated with the actual velocity. Hence, the migration-dip angle (ϕ) with the vertical can be computed as

$$\phi = \cos^{-1}\left(\frac{(\mathbf{P}_\mathrm{s} + \mathbf{P}_\mathrm{r}) \cdot \mathbf{z}}{|\mathbf{P}_\mathrm{s} + \mathbf{P}_\mathrm{r}|}\right), \qquad (1)$$

where **z** is a vertical unit vector.

Imaged data $I(\mathbf{X}, \phi, \psi)$, with the migration-dip (ϕ) and scattering (ψ) angles as the additional dimensions, can be efficiently produced using Kirchhoff migration (e.g., Hale, 1992). The conventional depth image $I(\mathbf{X})$ is obtained by summation over both ϕ and ψ. Dip-angle gathers $I(\mathbf{X}, \phi)$ are produced by summing over just the scattering angles (ψ), with the angle ϕ computed from equation 1.

In dip-angle CIGs created at the scatterer locations with the actual velocity parameters, reflections are curved, whereas diffractions are flat (Landa et al., 2008; Reshef and Landa, 2009). An appropriate taper function based on the normal vectors **n** can be applied to dip-angle gathers to mute the apex of the curved events, which suppresses reflections energy. Then stacking along the dip-angle axis enhances diffractions and yields a diffraction-based image.

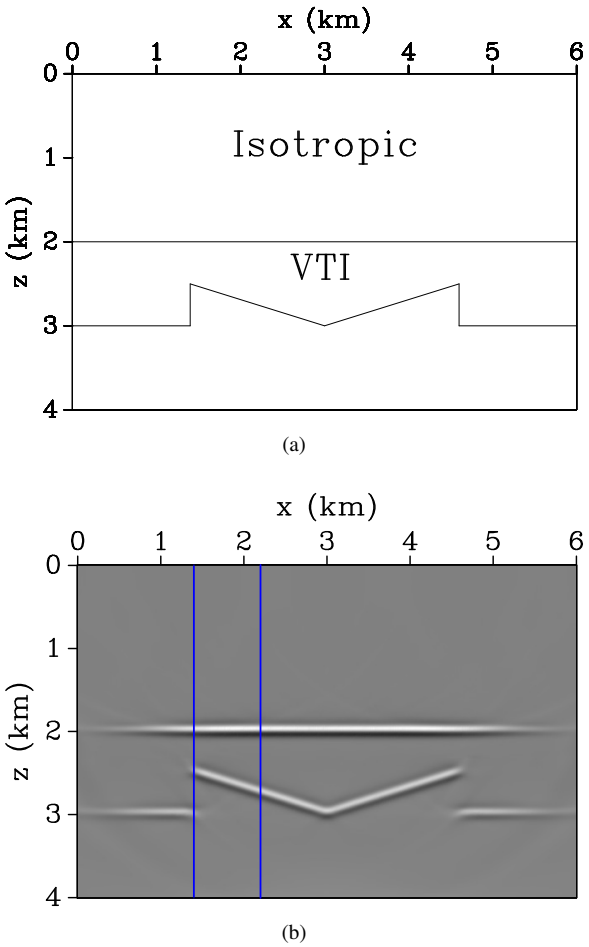

Figure 2. (a) VTI ramp model where the P-wave velocity in the isotropic layer is 3.1 km/s, and the Thomsen parameters of the VTI layer are $V_{P0} = 3.3$ km/s, $\epsilon = 0.24$, and $\delta = 0.14$. (b) A conventional Kirchhoff depth image for the model on plot (a) with the vertical blue lines marking CIG locations.

2.1 Numerical examples

We compute dip-angle CIGs for the diffraction ramp model in Figure 2a used by Arora and Tsvankin (2016). Two locations (vertical blue lines in Figure 2b) are chosen to analyze the signature of both specular reflections and nonspecular diffractions. The gather located at $x = 1.4$ km includes two scatterers (termination points of the interface segments) at depths close to $z = 2.5$ km and 3.0 km (Figure 3a). These scatterers pro-

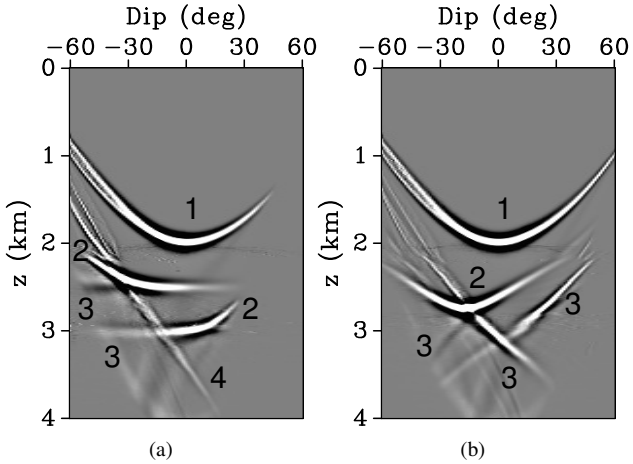

Figure 3. Dip-angle gathers for the ramp model in Figure 2a. (a) Gather at location $x = 1.4$ km. Event #1 is the reflection from the top of the VTI layer; events #2 are reflections from nearby interfaces; events #3 are diffractions from scatterers at the CIG location, and events #4 are diffractions from nearby scatterers. (b) Gather at location $x = 2.2$ km. Events #1 and #2 are reflections from the top and bottom of the VTI layer, respectively; events #3 are diffractions from nearby scatterers.

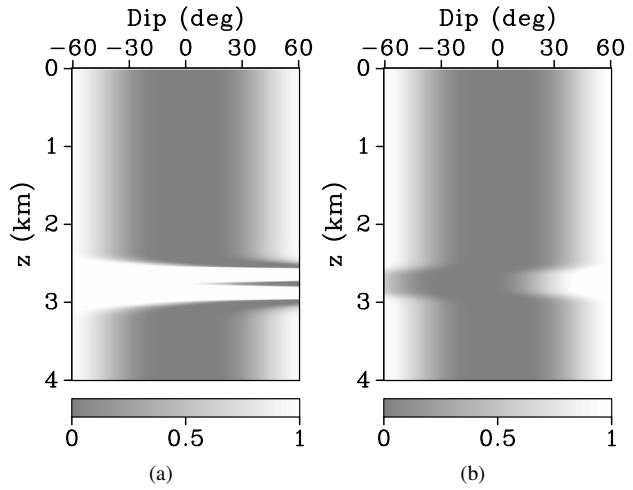

Figure 4. Mask for the dip-angle gathers in Figure 3.

duce relatively weak diffractions, which represent flat events because the velocity model is accurate. In contrast, the reflector at depth $z = 1.0$ km generates a strong curved event.

Only reflectors are present at location $x = 2.0$ km, and the corresponding reflection events in the dip-angle gather are curved (Figure 3b). Also, nearby interfaces produce additional curved reflection events with steep moveouts. The quasi-linear events in both gathers are diffractions from scatterers shifted laterally from the CIG location. The flatness of diffractions in dip-angle CIGs computed with an accurate velocity model

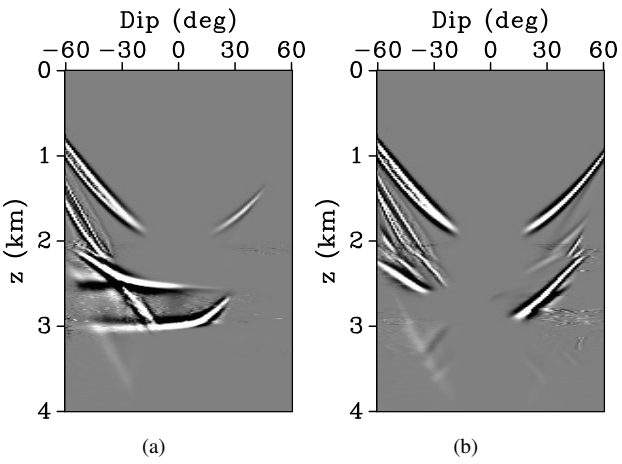

Figure 5. Dip-angle gathers from Figure 3 after applying the mask in Figure 4. Stacking along the dip-angle axis produces a diffraction-based image.

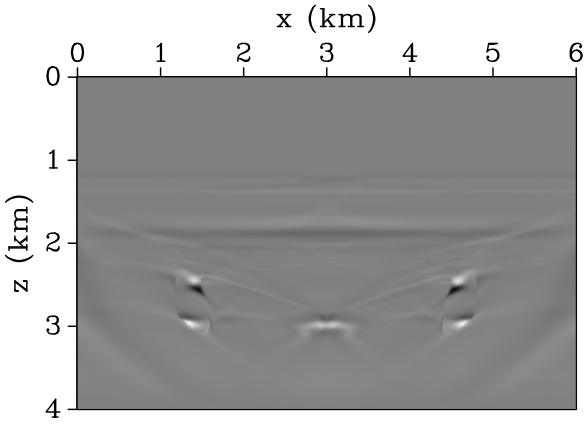

Figure 6. Diffraction-based depth image obtained from the dip-angle gathers in Figure 5.

allows one to separate them from reflections. Here, we use an apex removal technique to suppress reflection energy and produce a depth image just from diffractions.

The apex (or stationary point) of a curved reflection event in the dip-angle domain (e.g., see Figure 3) corresponds to the actual interface dip (Bleistein et al., 2013). As suggested by Klokov and Fomel (2012), we construct a mask (Figure 4) using dip information (vector **n**) to mute the reflections at their apex. Stacking along the dip axis after the reflections have been suppressed (Figure 5) produces a depth image from diffractions (Figure 6), which is comparable to that obtained by Arora and Tsvankin (2016) using a specularity-based method. It should be noted that the mask also mutes some of the diffraction energy, especially if diffraction events are curved due to velocity errors.

The main shortcoming of this method is its reliance on the accuracy of the velocity model. Therefore, application

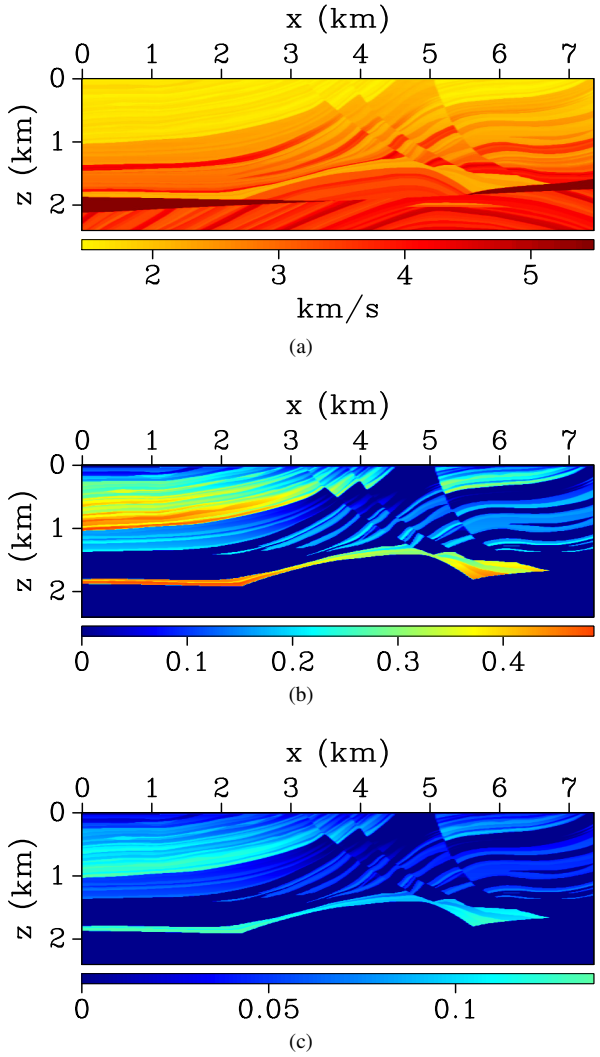

Figure 7. VTI Marmousi model: (a) the P-wave vertical velocity V_{P0} and the anisotropy coefficients (b) ϵ, and (c) δ.

of diffractions in velocity analysis may require a different separation technique.

Next, we apply this method of constructing diffraction-based images to the VTI version of the structurally complex Marmousi model (Alkhalifah, 1997). Several scatterers, created by the intersections of faults with layer boundaries (Figure 7), are not clearly visible on the conventional depth image (Figure 8a). A depth image from diffractions substantially enhances scatterers, albeit along with some residual reflection energy (Figure 8b).

3 VELOCITY ANALYSIS IN DIP-ANGLE GATHERS

The potential of dip-angle CIGs for separating diffractions and employing them in isotropic MVA was shown by Landa et al. (2008), Reshef and Landa (2009), and Klokov and Fomel (2012). A key step in implementing model updating (MVA) using diffractions is their separation from reflections when the velocity field is still inaccurate.

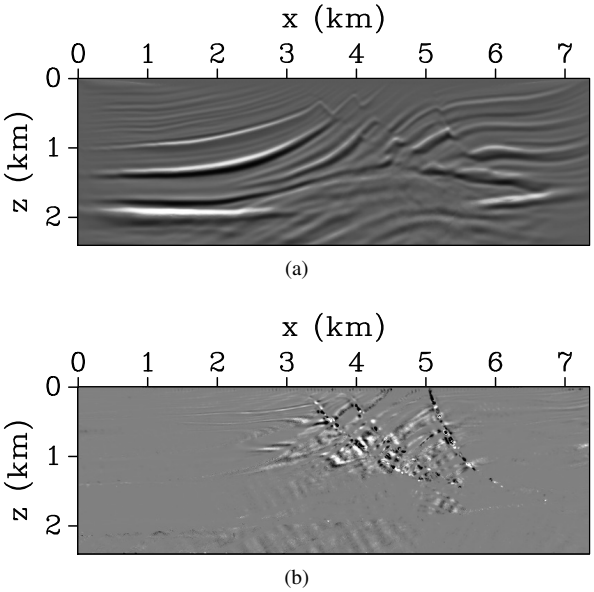

Figure 8. (a) Conventional (reflection-based), and (b) diffraction-based depth images for the model in Figure 7. Both images are computed with the actual velocity model.

3.1 Properties of dip-angle CIGs

Here, we analyze dip-angle gathers for the VTI model in Figure 9, which includes a point scatterer along with dipping and horizontal reflectors. Our goal is to assess the influence of errors in the P-wave zero-dip NMO velocity V_{nmo}, the anellipticity parameter η, and Thomsen parameter δ on the reflection and diffraction events in the dip-angle domain. As discussed by Alkhalifah and Tsvankin (1995) and Tsvankin (2012), the parameters V_{nmo} and η are primarily responsible for focusing reflections in time and depth migration for VTI media, while δ controls migrated reflector depths.

Indeed, errors in V_{nmo} and η for the model in Figure 9 cause residual moveout for the diffraction from the scatterer at $z = 1$ km, while reflections maintain their curved shape (Figures 10 and 11). Note that inaccurate values of V_{nmo} produce residual moveout for diffractions at almost all dip angles, while the residual moveout due to errors in η becomes pronounced at relatively large dips. Such a behaviour is expected because the influence of η on the NMO velocity of dipping events increases with dip (Tsvankin, 2012). In contrast, δ-errors distort the imaged depths of the scatterer and reflectors but do not produce residual moveout for the diffraction events (Figure 12). The curvature of the reflection events remains almost unchanged for the actual and distorted velocity models. Therefore, dip-angle domain is not suitable to perform MVA of reflection data.

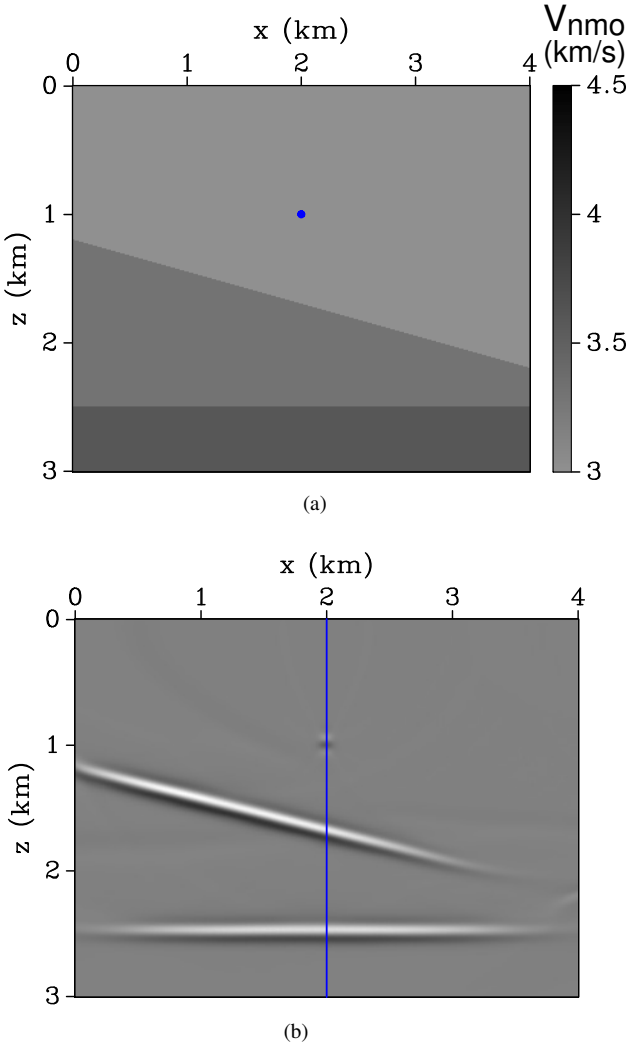

Figure 9. (a) Layered VTI model with $V_{nmo} = 3.28$ km/s in the overburden and 3.61 km/s in the dipping layer. The anisotropy parameters $\eta = 0.22$ and $\delta = 0.10$ are the same in both layers. (b) A conventional depth image with the vertical blue line marking the CIG location.

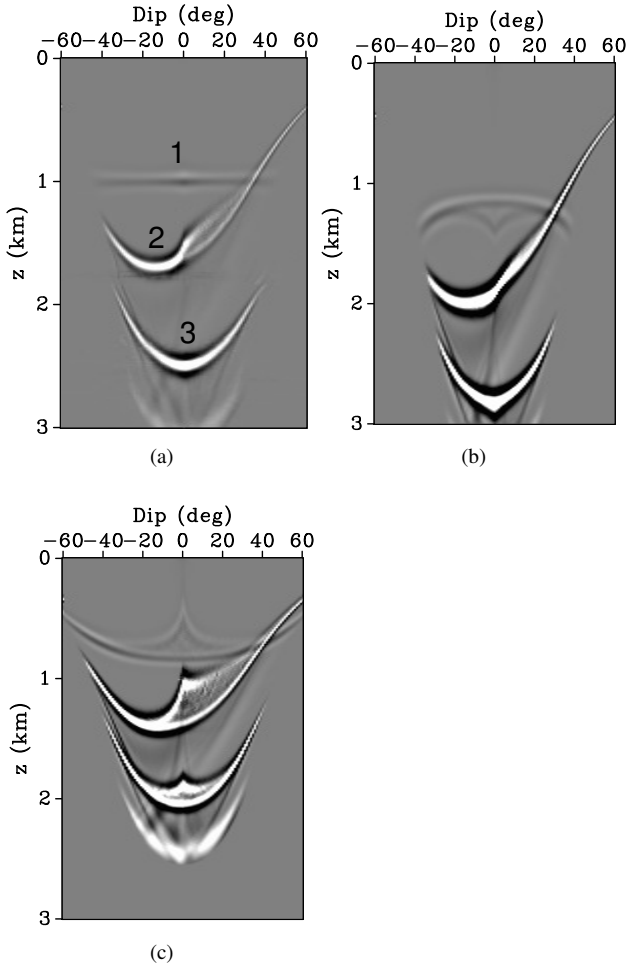

Figure 10. Dip-angle CIGs for the model in Figure 9 at $x = 2.0$ km computed with the (a) actual velocity field; (b) overstated $V_{nmo} = 3.77$ km/s (constant throughout the model); and (c) understated constant $V_{nmo} = 2.79$ km/s. Event #1 is the diffraction from the scatterer and events #2 and #3 are reflections.

3.2 MVA using diffractions

Reshef and Landa (2009) and Klokov and Fomel (2012) use velocity-scanning methods to perform isotropic MVA of diffraction events in dip-angle gathers. This approach may not be practical for anisotropic parameter estimation because it is computationally expensive for field data and does not account for realistic lateral heterogeneity. Also, it is necessary to estimate the locations of the scatterers from the diffraction-based depth images. Knowledge of those locations is needed to construct dip-angle CIGs, which provide the input for the tomographic model updating.

Instead of velocity scanning, we propose to use residual moveout of diffractions in dip-angle gathers to refine the anisotropic velocity field. The residual moveout of reflected waves in surface-offset CIGs has been widely used in MVA and reflection tomography to build isotropic and TI velocity models (e.g., Liu, 1997; Sarkar and Tsvankin, 2004; Woodward et al., 2008; Wang and Tsvankin, 2013). Efficient separation of diffractions that preserves their residual moveout in dip-angle CIGs is a necessary condition for diffraction-based velocity analysis. Therefore, the initial model (presumably obtained from reflections) should be sufficiently accurate so that reflections could be effectively suppressed without significantly damaging diffractions events. Velocity updates obtained through the diffraction-based anisotropic MVA should improve the focusing of scatterers in depth images and, potentially, the quality of reflection-based images.

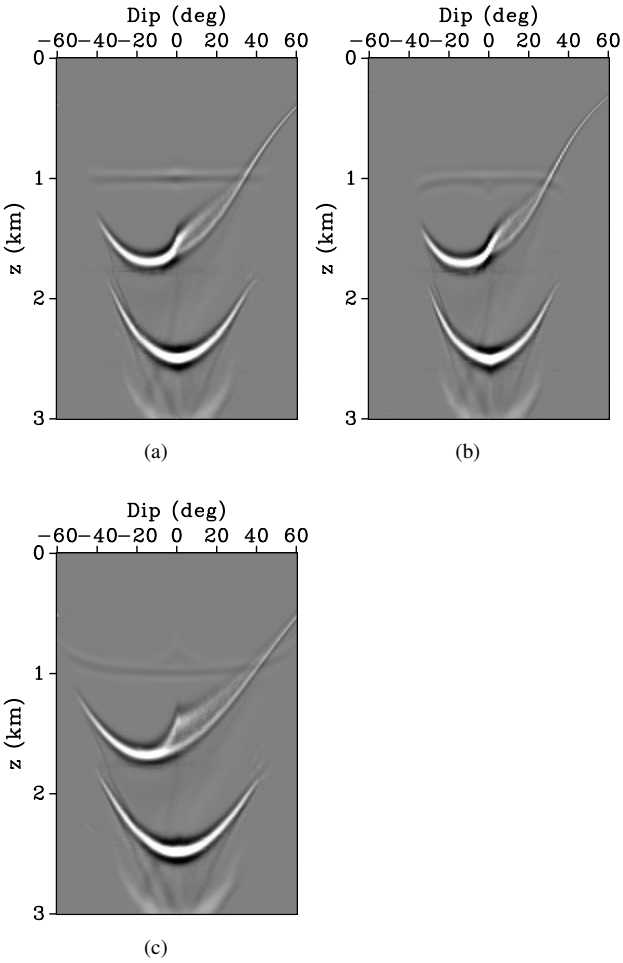

Figure 11. Dip-angle CIGs for the model in Figure 9 at $x = 2.0$ km computed with the (a) actual velocity field; (b) overstated $\eta = 0.37$ (constant throughout the model); and (c) understated constant $\eta = 0.07$.

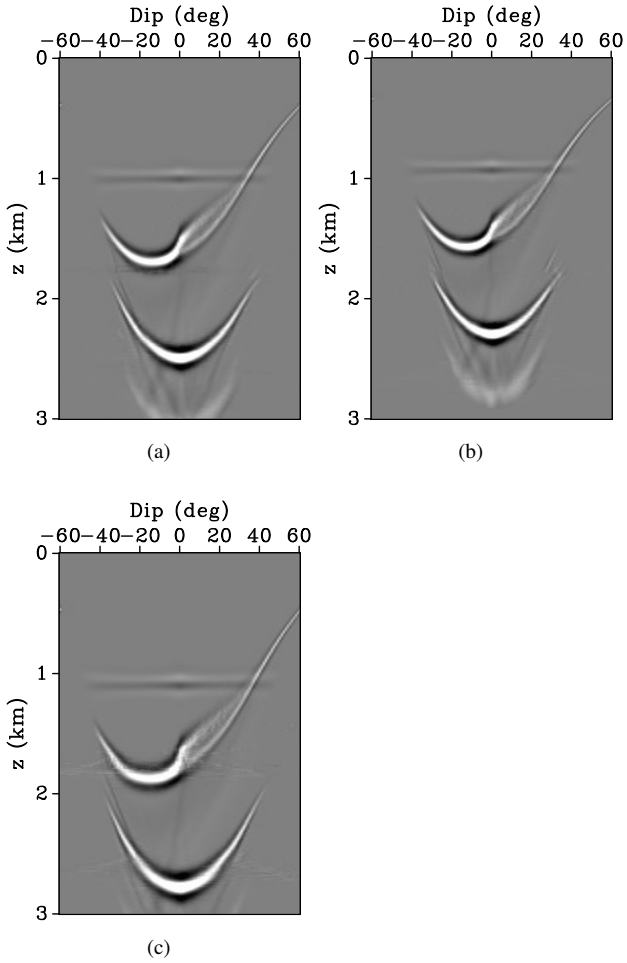

Figure 12. Dip-angle CIGs for the model in Figure 9 at $x = 2.0$ km computed with the (a) actual velocity field; (b) overstated $\delta = 0.20$ (constant throughout the model); and (c) understated constant $\delta = 0$.

4 CONCLUSIONS

We proposed to implement diffraction-based imaging and velocity analysis in TI media using dip-angle common-image-gathers. These gathers can be generated by Kirchhoff depth migration with subsequent summation over scattering angles. If migration is performed with an accurate velocity field, diffractions in dip-angle CIGs are flat, whereas reflections are curved. Hence, reflections events can be muted using a simple mask computed from the interface normal vectors. We applied this technique to a VTI ramp and Marmousi models to produce a diffraction-based depth images from dip-angle gathers. However, separation of diffractions based on the shape of their moveout may fail in the presence of velocity errors.

To analyze the sensitivity of diffractions and reflections in dip-angle domain to velocity distortions, we perturbed the parameters $V_{\rm nmo}$, η and δ of a layered VTI medium. Residual moveout developed by diffractions for inaccurate values of $V_{\rm nmo}$ and η could be used in a tomographic algorithm to update the TI models. Errors in the NMO velocity produce residual moveout at almost all dips, whereas the influence of η becomes substantial at relatively large dip angles. Errors in δ distort only the depths of the imaged events in our test; however, a laterally varying δ-field above a scatterer could generate residual moveout for the corresponding diffraction. In contrast, the moveout of reflections in dip-angle gathers does not provide suitable criteria for model updating. Ongoing work includes MVA of diffractions in dip-angle gathers with the goal of refining the parameters $V_{\rm nmo}$ and η.

5 ACKNOWLEDGMENTS

We would like to thank the members of the A(anisotropy)-Team for useful discussions and Vladimir Li of CWP for providing TI acoustic modeling codes. This work was supported by the Consortium Project on Seismic Inverse Methods for

Complex Structures at CWP. The reproducible numerical examples in this report are generated with the Madagascar open-source software package (Fomel et al., 2013) freely available from http://www.ahay.org.

REFERENCES

Al-Dajani, A., and S. Fomel, 2010, Fractures detection using multi-azimuth diffractions focusing measure: Is it feasible?: 80th Annual International Meeting, SEG, Expanded Abstracts, 287–291.

Alkhalifah, T., 1997, An anisotropic marmousi model: SEP-95: Stanford Exploration Project, 265–282.

Alkhalifah, T., and I. Tsvankin, 1995, Velocity analysis for transversely isotropic media: Geophysics, **60**, 1550–1566.

Alonaizi, F., R. Pevzner, A. Bona, M. Alshamry, E. Caspari, and B. Gurevich, 2014, Application of diffracted wave analysis to time-lapse seismic data for CO_2 leakage detection: Geophysical Prospecting, **62**, 197–209.

Arora, Y., and I. Tsvankin, 2016, Separation of diffracted waves in transversely isotropic media: Studia Geophysica et Geodaetica, **60**, 487–499.

Audebert, F., P. Froidevaux, H. Rakotoarisoa, J. S. Lucas, et al., 2002, Insights into migration in the angle domain: 72nd Annual International Meeting, SEG, Expanded Abstracts.

Berkovitch, A., I. Belfer, Y. Hassin, and E. Landa, 2009, Diffraction imaging by multifocusing: Geophysics, **74**, no. 6, WCA75–WCA81.

Billette, F., S. L. Bégat, P. Podvin, and G. Lambaré, 2003, Practical aspects and applications of 2D stereotomography: Geophysics, **68**, 1008–1021.

Bleistein, N., J. K. Cohen, and J. W. Stockwell Jr., 2013, Mathematics of multidimensional seismic imaging, migration, and inversion: Springer Science & Business Media, **13**.

Brandsberg-Dahl, S., B. Ursin, and M. De Hoop, 2003, Seismic velocity analysis in the scattering-angle/azimuth domain: Geophysical Prospecting, **51**, 295–314.

De Vries, D., and A. Berkhout, 1984, Velocity analysis based on minimum entropy: Geophysics, **49**, 2132–2142.

Fomel, S., E. Landa, and M. Taner, 2007, Poststack velocity analysis by separation and imaging of seismic diffractions: Geophysics, **56**, no. 6, U89–U94.

Fomel, S., P. Sava, I. Vlad, Y. Liu, and V. Bashkardin, 2013, Madagascar: Open-source software project for multidimensional data analysis and reproducible computational experiments: Journal of Open Research Software, **1**.

Hale, D., 1992, Migration by the Kirchhoff, slant stack, and Gaussian beam methods: CWP Project Review Report.

Harlan, W. S., J. F. Claerbout, and F. Rocca, 1984, Signal/noise separation and velocity estimation: Geophysics, **49**, 1869–1880.

Khaidukov, V., E. Landa, and T. J. Moser, 2004, Diffraction imaging by focusing-defocusing: An outlook on seismic superresolution: Geophysics, **69**, 1478–1490.

Klem-Musatov, K. D., F. Hron, L. R. Lines, and C. A. Meeder, 1994, Theory of seismic diffractions: Society of Exploration Geophysicists Tulsa, USA.

Klokov, A., and S. Fomel, 2012, Separation and imaging of seismic diffractions using migrated dip-angle gathers: Geophysics, **77**, no. 6, S131–S143.

Kozlov, E., N. Barasky, E. Korolev, A. Antonenko, and E. Koshchuk, 2004, Imaging scattering objects masked by specular reflections: 74th Annual International Meeting, SEG, Expanded Abstracts, 1131–1134.

Landa, E., S. Fomel, and M. Reshef, 2008, Separation, imaging, and velocity analysis of seismic diffractions using migrated dip-angle gathers: 78th Annual International Meeting, SEG, Expanded Abstracts.

Liu, Z., 1997, An analytical approach to migration velocity analysis: Geophysics, **62**, 1238–1249.

Moser, T., and C. Howard, 2008, Diffraction imaging in depth: Geophysical Prospecting, **56**, 627–641.

Reshef, M., and E. Landa, 2009, Post-stack velocity analysis in the dip-angle domain using diffractions: Geophysical Prospecting, **57**, 811–821.

Sarkar, D., and I. Tsvankin, 2004, Migration velocity analysis in factorized VTI media: Geophysics, **69**, 708–718.

Sava, P. C., B. Biondi, and J. Etgen, 2005, Wave-equation migration velocity analysis by focusing diffractions and reflections: Geophysics, **70**, U19–U27.

Söllner, W., W. Yang, et al., 2002, Diffraction response simulation: a 3D velocity inversion tool: 72nd Annual International Meeting, SEG, Expanded Abstracts, 2293–2296.

Sturzu, I., A. M. Popovici, N. Tanushev, I. Musat, M. A. Pelissier, and T. J. Moser, 2013, Specularity gathers for diffraction imaging: 75th EAGE Conference & Exhibition, Extended Abstracts.

Tsvankin, I., 2012, Seismic signatures and analysis of reflection data in anisotropic media, 3rd edition: Society of Exploration Geophysicists.

Waheed, U. B., T. Alkhalifah, and A. Stovas, 2013a, Diffraction traveltime approximation for TI media with an inhomogeneous background: Geophysics, **78**, no. 5, WC103–WC111.

Waheed, U. B., A. Stovas, and T. Alkhalifah, 2013b, Anisotropic parameter inversion in VTI media using diffraction data: 83rd Annual International Meeting, SEG, Expanded Abstracts.

Wang, X., and I. Tsvankin, 2013, Multiparameter TTI tomography of P-wave reflection and VSP data: Geophysics, **78**, no. 5, WC51–WC63.

Woodward, M. J., D. Nichols, O. Zdraveva, P. Whitfield, and T. Johns, 2008, A decade of tomography: Geophysics, **73**, no. 5, VE5–VE11.